

AD/A-000 933

OCULAR EFFECTS OF ULTRAVIOLET LASER RADIATION

TECHNOLOGY, INCORPORATED

PREPARED FOR
SCHOOL OF AEROSPACE MEDICINE

SEPTEMBER 1974

DISTRIBUTED BY:

NTIS

National Technical Information Service
U. S. DEPARTMENT OF COMMERCE

NOTICES

This interim report was submitted by Technology Inc., 8531 North New Braunfels Avenue, San Antonio, Texas 78217, under contract F41609-73-C-0017, job order 6301-05-34, with the USAF School of Aerospace Medicine, Aerospace Medical Division, AFSC, Brooks Air Force Base, Texas. Major James T. Gallagher (SAM/RAL) was the Laboratory Project Scientist-in-Charge.

When U.S. Government drawings, specifications, or other data are used for any purpose other than a definitely related Government procurement operation, the Government thereby incurs no responsibility nor any obligation whatsoever; and the fact that the Government may have formulated, furnished, or in any way supplied the said drawings, specifications, or other data is not to be regarded by implication or otherwise, as in any manner licensing the holder or any other person or corporation, or conveying any rights or permission to manufacture, use, or sell any patented invention that may in any way be related thereto.

This report has been reviewed and cleared for open publication and/or public release by the appropriate Office of Information (OI) in accordance with AFR 190-17 and DODD 5230.9. There is no objection to unlimited distribution of this report to the public at large, or by DDC to the National Technical Information Service (NTIS).

This technical report has been reviewed and is approved for publication.

James T. Gallagher
JAMES T. GALLAGHER, Major, USAF
Project Scientist-in-Charge

Evan R. Golera
EVAN R. GOLERA, Colonel, USAF, MC
Commander

ACCESSION for	
NTIS	White Section <input checked="" type="checkbox"/>
DIC	Buff Section <input type="checkbox"/>
UNCLASSIFIED	<input type="checkbox"/>
JUSTIFICATION	
BY	
DISTRIBUTION/AVAILABILITY CODES	
Dist.	ATL. and/or SPECIAL
A	

UNCLASSIFIED

SECURITY CLASSIFICATION OF THIS PAGE (When Data Entered)

REPORT DOCUMENTATION PAGE		READ INSTRUCTIONS BEFORE COMPLETING FORM
1. REPORT NUMBER SAM-TR-74-32	2. GOVT ACCESSION NO.	3. RECIPIENT'S CATALOG NUMBER AD/A-000933
4. TITLE (and Subtitle) OCULAR EFFECTS OF ULTRAVIOLET LASER RADIATION		5. TYPE OF REPORT & PERIOD COVERED Interim Report Feb. 1973 - Feb. 1974
		6. PERFORMING ORG. REPORT NUMBER
7. AUTHOR(s) Joseph Zuclich, Ph.D.		8. CONTRACT OR GRANT NUMBER(s) F41609-73-C-0017
9. PERFORMING ORGANIZATION NAME AND ADDRESS Technology Incorporated 8531 N. New Braunfels Avenue San Antonio, Texas 78217		10. PROGRAM ELEMENT, PROJECT, TASK AREA & WORK UNIT NUMBERS 62202F 6301-05-34
11. CONTROLLING OFFICE NAME AND ADDRESS USAF School of Aerospace Medicine (RAL) Aerospace Medical Division (AFSC) Brooks Air Force Base, Texas 78235		12. REPORT DATE September 1974
		13. NUMBER OF PAGES 29
14. MONITORING AGENCY NAME & ADDRESS (if different from Controlling Office)		15. SECURITY CLASS. (of this report) Unclassified
		15a. DECLASSIFICATION/DOWNGRADING SCHEDULE
16. DISTRIBUTION STATEMENT (of this Report) Approved for public release; distribution unlimited		
17. DISTRIBUTION STATEMENT (of the abstract entered in Block 20, if different from Report)		
18. SUPPLEMENTARY NOTES Reproduced by NATIONAL TECHNICAL INFORMATION SERVICE U.S. Department of Commerce Springfield, VA 22151		
19. KEY WORDS (Continue on reverse side if necessary and identify by block number) Laser Ultraviolet radiation Photochemistry Ocular hazard Corneal damage PRICES SUBJECT TO CHANGE		
20. ABSTRACT (Continue on reverse side if necessary and identify by block number) This report presents an analysis of ocular hazards from ultraviolet laser radiation. Absorption properties of primate-eye components are reviewed, cellular structure and molecular composition of pertinent ocular layers discussed, and absorption of these layers explained in terms of their molecular properties. Potential sites of ocular damage from various UV-wavelength ranges are identified.		

DD FORM 1 JAN 73 1473

EDITION OF 1 NOV 65 IS OBSOLETE

UNCLASSIFIED

SECURITY CLASSIFICATION OF THIS PAGE (When Data Entered)

OCULAR EFFECTS OF ULTRAVIOLET LASER RADIATION

INTRODUCTION

Ultraviolet laser systems are commercially available, and widespread use of these as well as systems still under development is anticipated in the near future. Although the biological systems' inherent sensitivity to UV radiation has long been recognized, safety standards developed for noncoherent UV sources are minimal and do not anticipate the range of parameters associated with laser systems. For example, there is little background for meaningful safety standards for such situations as high-intensity, short-pulsewidth UV exposures or repetitive pulse exposures. Therefore, there is a critical need to analyze the nature of damage that UV lasers can cause in living matter and to provide guidelines for protection against such damage. The need is especially acute with regard to ocular exposures where grave personnel hazards are created by low damage thresholds coupled with high potential for accidental exposure due to the victim not having any immediate physical awareness of the exposure.

The UV segment of the electromagnetic spectrum is somewhat arbitrarily divided into three wavelength regions--commonly called the near UV (300-400 nm), far UV (200-300 nm), and vacuum UV (4-200 nm). This investigation will deal specifically with ocular hazards from near- and far-UV radiation. In these wavelength regions, radiation is absorbed by chromophoric sites of proteins and nucleic acids. These chromophores are "aromatic" molecules characterized by delocalization or sharing of electrons by several chemical bonds, resulting in low-lying electronic energy levels.

The energy of a single photon in the near- or far-UV wavelength range may promote an electron of the absorbing aromatic chromophores to an excited energy level. The excited state, which the absorbing molecule then finds itself in, is highly labile, and the molecule may engage in any number of photochemical reactions. The resulting photo-induced products may be incompatible with the normal functioning of the exposed system and, in time, may lead to biological damage observable on the macroscopic level.

The photochemical damage mechanism appears to be most efficient in the 260- to 280-nm wavelength range, where many living systems exhibit maximum sensitivity to UV radiation. This wavelength range coincides with the first absorption bands

of the chromophoric absorbing sites of all proteins and nucleic acids. The photochemical mechanism is the dominant source of radiation damage only over a limited wavelength range, tentatively estimated to be $\approx 200\text{-}340\text{ nm}$. At longer wavelengths, the energy of a single photon is not sufficient to induce excited electronic states in the normal constituents of proteins and amino acids. At shorter wavelengths, radiation is no longer selectively absorbed by the photosensitive aromatic chromophores; instead, it is absorbed by more sites in the biological material, many of which are more photoresistive than the aromatic molecules and may disperse the absorbed energy in a less damaging manner. At still shorter wavelengths, direct ionization becomes the dominant form of radiation damage. Since extensive literature is available on ionizing radiation and sophisticated models have already been developed to deal with this aspect of radiation damage, it is not considered further herein.

In this report the absorption properties of the primate-eye components are reviewed and used to anticipate potential damage sites from radiation in the wavelength range $200\text{-}400\text{ nm}$. The cellular structure of the cornea is discussed along with the molecular composition of the various corneal layers. (UV damage over most of the $200\text{-}400\text{-nm}$ range is restricted to the cornea.) Absorption properties of individual aromatic molecules are presented, and UV-radiation absorption by living tissue is explained in terms of these molecular properties.

UV ABSORPTION BY THE PRIMATE EYE

The transmission of the individual ocular media of primate eyes has been determined by Boettner (2) for wavelengths of 220 nm through 2.8μ . His data have been used to plot percent absorption vs. wavelength for the cornea, aqueous humor, lens, and vitreous humor of the rhesus monkey (Fig. 1) and the human (Fig. 2). The rabbit, rhesus, and human cornea compositions are very similar. Unless otherwise stated, corneal properties discussed here will apply to all of these species.

The cornea absorbs virtually all incident radiation below 280 nm . Above 280 nm , the cornea becomes partially transmissive, but the lens continues to absorb strongly throughout the remainder of the UV range. The low percentage of near-UV radiation transmitted through the lens will be absorbed by the pigment epithelium layer of the retina. The aqueous and vitreous humors are ineffective absorbers of wavelengths not screened by anterior components of the eye.

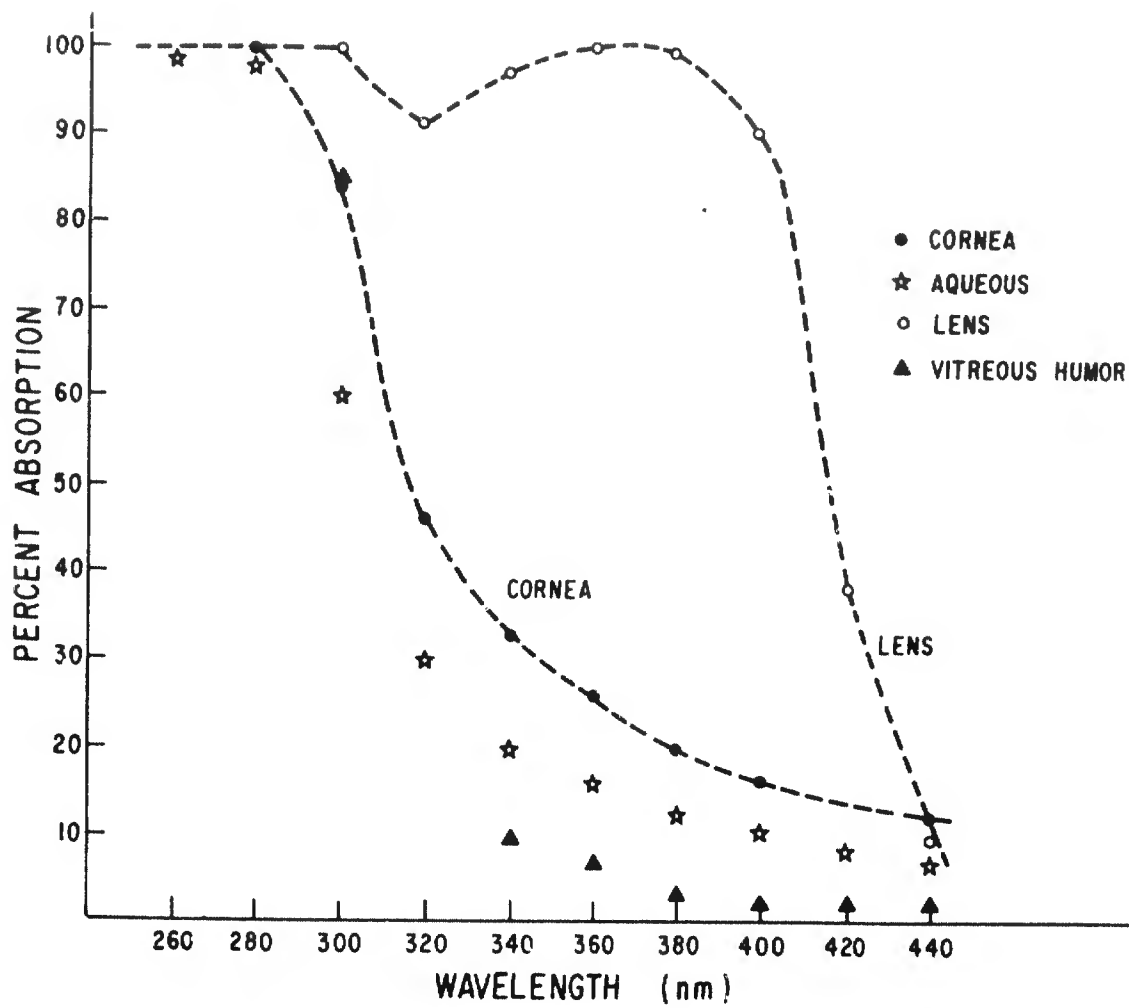


Figure 1. Absorption spectra of rhesus-eye components.

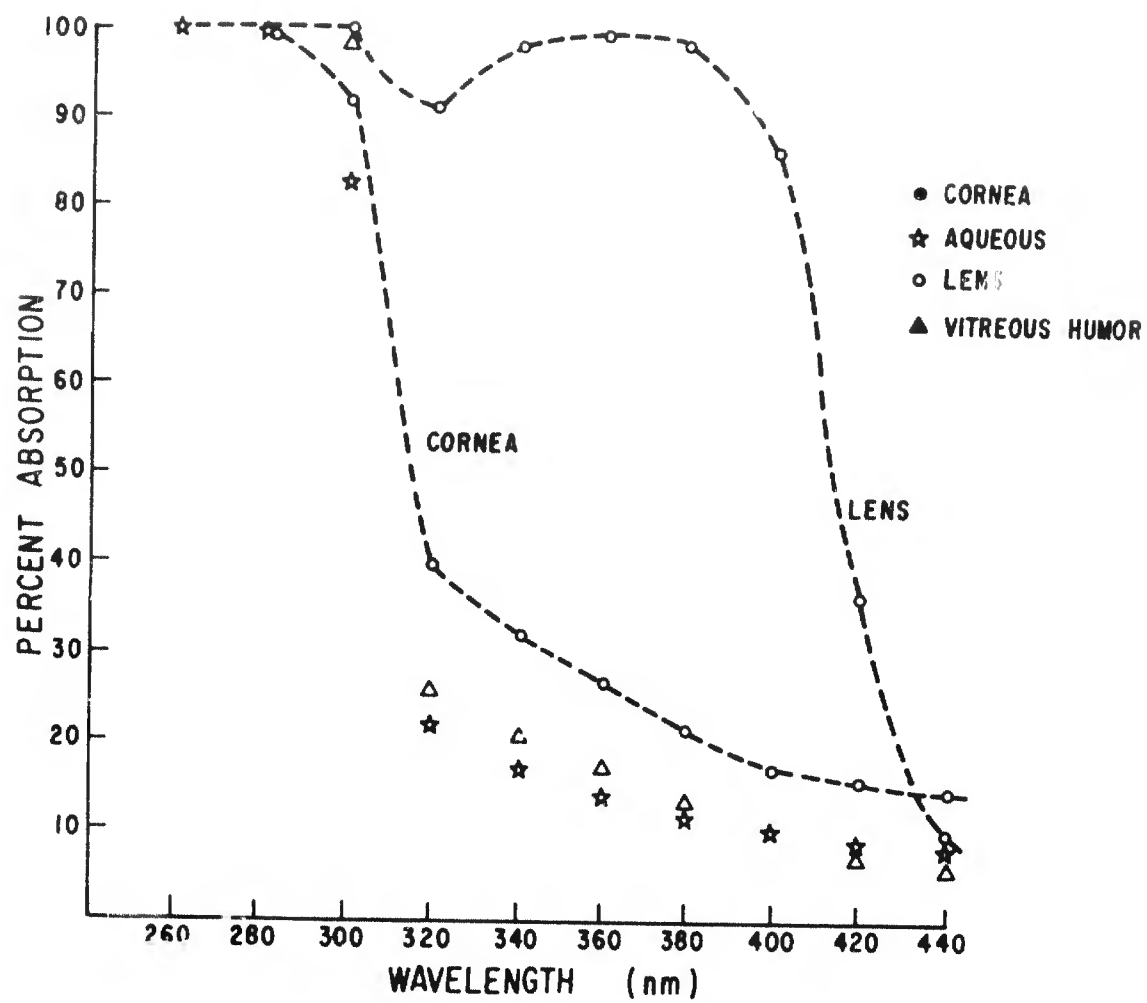


Figure 2. Absorption spectra of human-eye components.

Ocular damage from far-UV radiation is expected to be restricted to the cornea. Further, over most of the far-UV range, lesions appear only in the corneal epithelium--approximately the outer 10% of the total thickness of the cornea. Figure 3 illustrates that the epithelium layer absorbs most incident radiation below 280 nm (9).

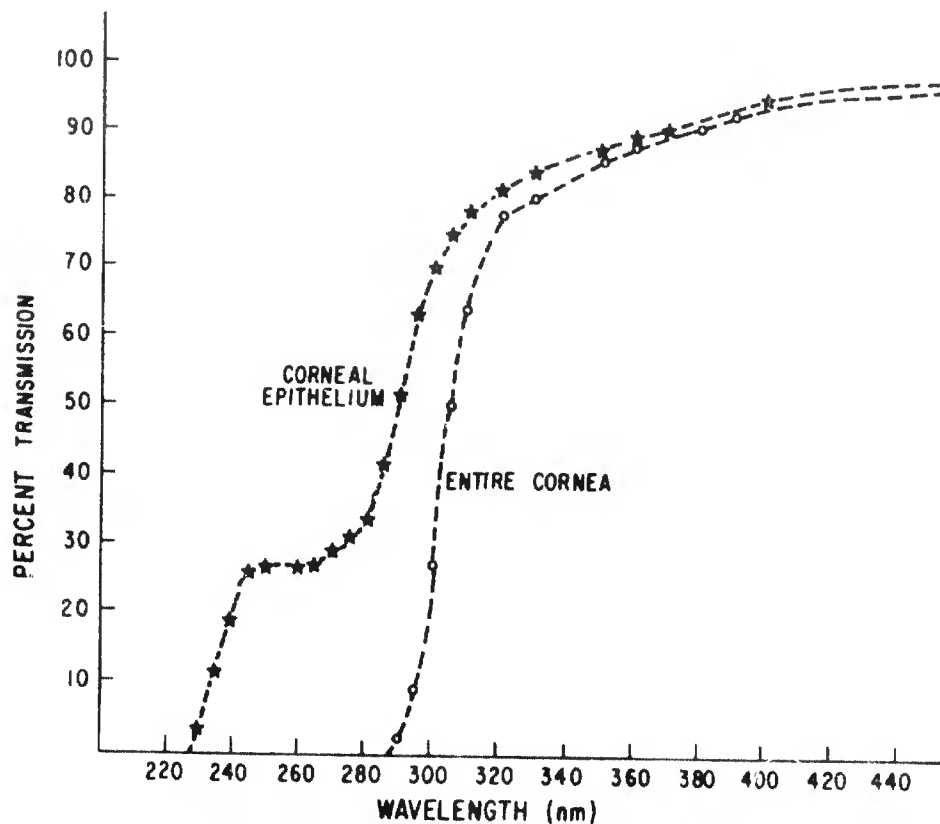


Figure 3. Transmission spectra of the cornea (rabbit).

The action spectrum for photokeratitis in the rabbit eye due to exposure to noncoherent UV radiation is shown in Figure 4 (14). No comparable data are available on exposures to coherent UV radiation. Theoretically, there is no basis for expecting differences due to the property of coherence in the interactions of UV radiation with living matter.

Although epithelial radiation damage may be temporarily incapacitating, it is completely repairable and full visual recovery occurs in a matter of days. At higher intensities of incident UV radiation, lesions may also be formed in the

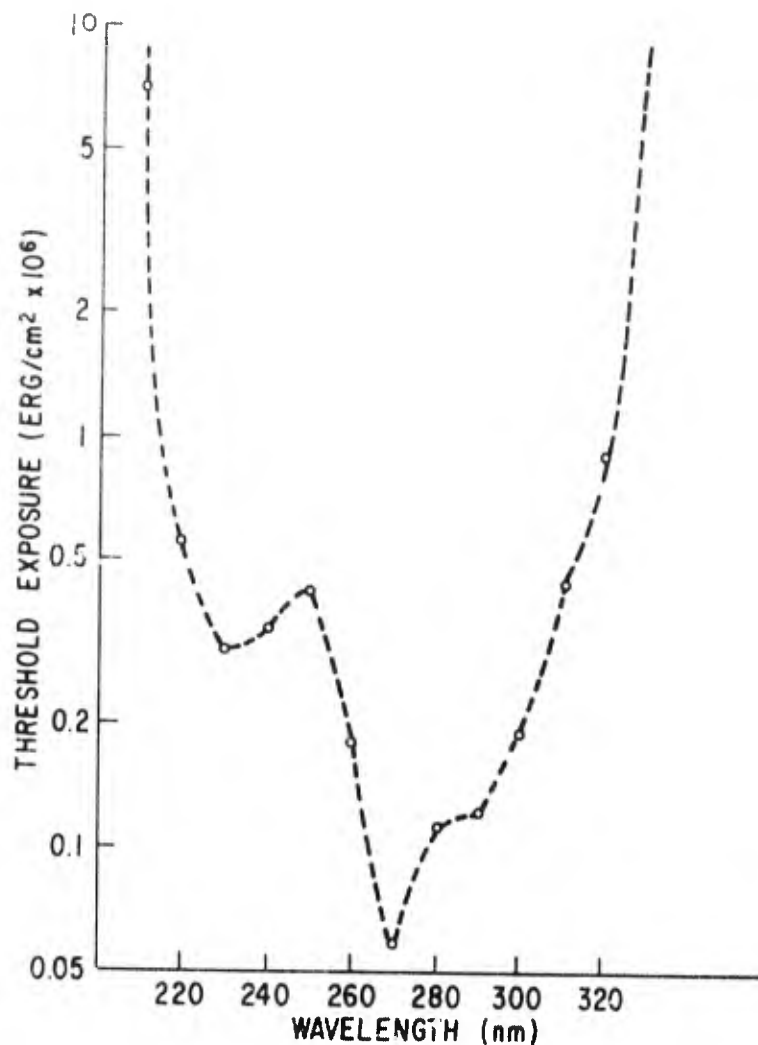


Figure 4. Action spectrum for photokeratitis for rabbits.

posterior layers of the cornea. Such injury usually results in scar formation, and the resulting opacities, if of sufficient size, cause permanent loss of visual acuity. Thus, at UV wavelengths where the epithelium is partially transparent, it is important to determine an action spectrum for corneal scarring. Quantitative data for this type of damage have not appeared in the literature.

The lens absorbs most UV radiation transmitted through the cornea. In addition to the aromatic molecules found in the cornea, the lens contains a yellowish pigment with an absorption peak in the near-UV range (4). The lens optical density has been measured in several species and the results for the rhesus monkey and the human are seen in Figure 5.

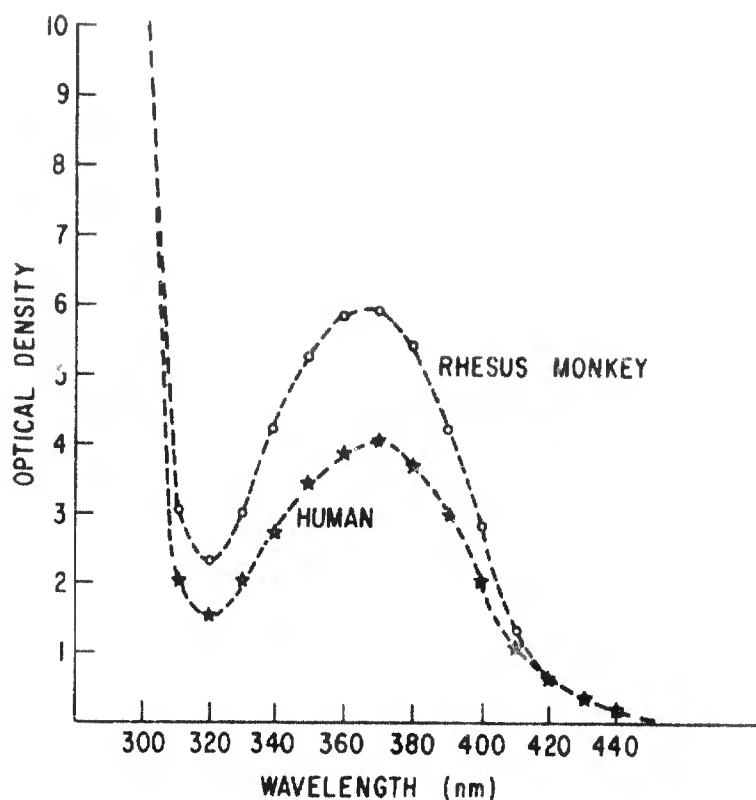


Figure 5. Density spectra of primate lenses.

In the near UV range, absorption maxima are found at 366 nm and minima at 320 nm. The minima allow approximately 1% of the light incident upon the cornea to be transmitted directly to the retina at 320 nm. A similar percentage of incident radiation reaches the retina at 400 nm. Above 400 nm this percentage increases very rapidly with wavelength.

Since most incident radiation at 366 nm is absorbed by the lens, is the lens the primary site of damage from this wavelength radiation? If so, over what wavelength range is the lens the eye's most sensitive component? Unfortunately, little quantitative data are available on lenticular damage in the near UV. Broadband radiation in the vicinity of 300 nm indicates comparable thresholds for lenticular and corneal damage when using reversible lens clouding as a damage criterion (1). The only useful piece of data, however, is a result indicating that the threshold for cataract formation at 325 nm is roughly eight times the threshold value of 31.6 joule/cm² found for corneal damage at this wavelength (6).

On the basis of the preliminary results for 325-nm radiation, the lens and cornea may be expected to have comparable thresholds for damage at 366 nm. More incident radiation is transmitted through the cornea at 366 nm than at 325 nm, and the radiation which reaches the lens is absorbed more strongly at 366 nm. Quantitatively, the absorption characteristics (Figs. 3 and 5) can be used to predict a decrease by a factor of 6.9 in the relative thresholds for lenticular to corneal damage in going from 325 nm to 366 nm. (This calculation is only meaningful if the mechanism for damage and its efficiency does not change over the wavelength range in question.)

The result for lens damage at 325 nm represents a gross form of lens damage--cataract formation, observed within a matter of hours after irradiation. With lower levels of irradiation, cataract formation may not be apparent until many months after the exposure, but the end result is still serious ocular damage. Thus, it seems imperative to consider the lens as a potential site for damage over part of the near-UV range and to establish a suitable criterion for predicting long-term cataract formation.

With visible light, most incident radiation is transmitted to the retina, and the dominant mechanism for damage is believed to be a thermal effect. As the wavelength is shortened to 400 nm and into the near UV, a much smaller percentage of radiation reaches the retina; nevertheless, at this wavelength the retina may be the most sensitive component of the eye. In any event, the threshold for retinal damage will vary considerably near 400 nm. Figure 6 shows that, at this wavelength, the percent of incident radiation transmitted through the anterior components to the retina varies radically (1). (By way of contrast, there is little wavelength dependence from 450 to 800 nm.)

CELLULAR COMPOSITION OF THE CORNEA

A transverse section of the human cornea is depicted in Figure 7 (5, 10). The human, rhesus, and rabbit corneas are similar except the rabbit has no Bowman's membrane.

The surface layer, or epithelium, comprises about 10% of the cornea's total thickness. A closeup view (Fig. 8) shows five or six layers of cells, divided into three categories in the epithelium. Its posterior border is lined by a layer of basal, or columnar cells. These cells have oval nuclei with the long axis perpendicular to the corneal surface. Above the basal layer are two layers of polyhedral cells, elongated and oriented parallel to the surface. Finally,

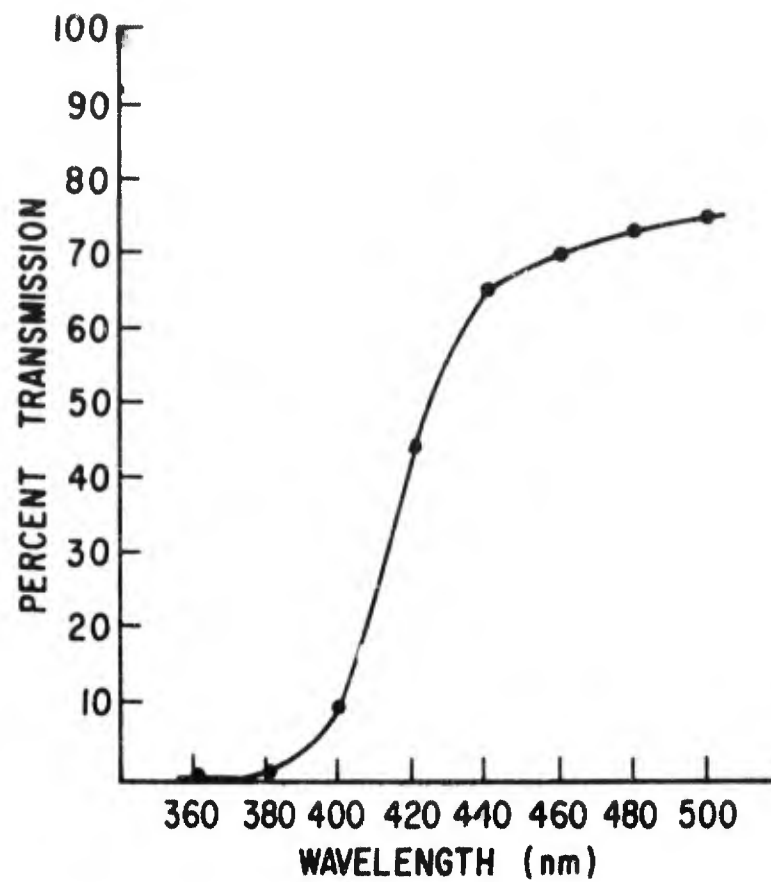


Figure 6. Percent of corneal incident radiation transmitted to retina.

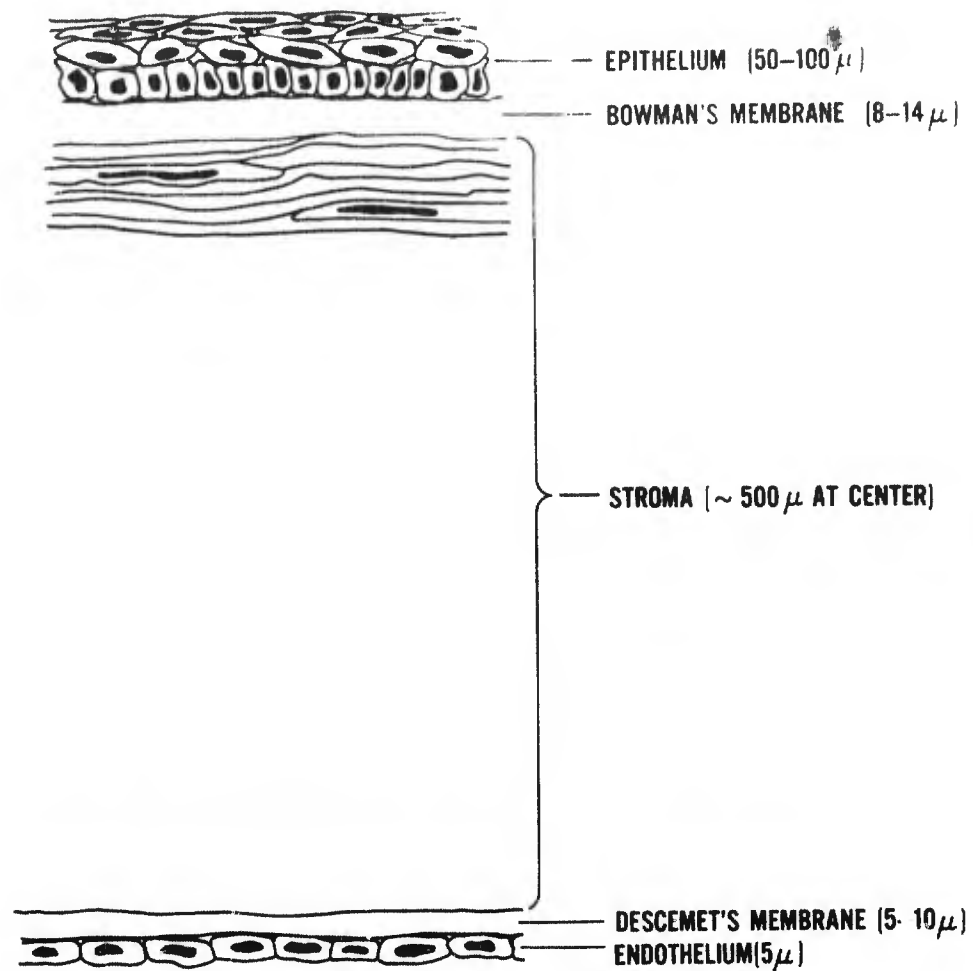


Figure 7. Transverse section of cornea.

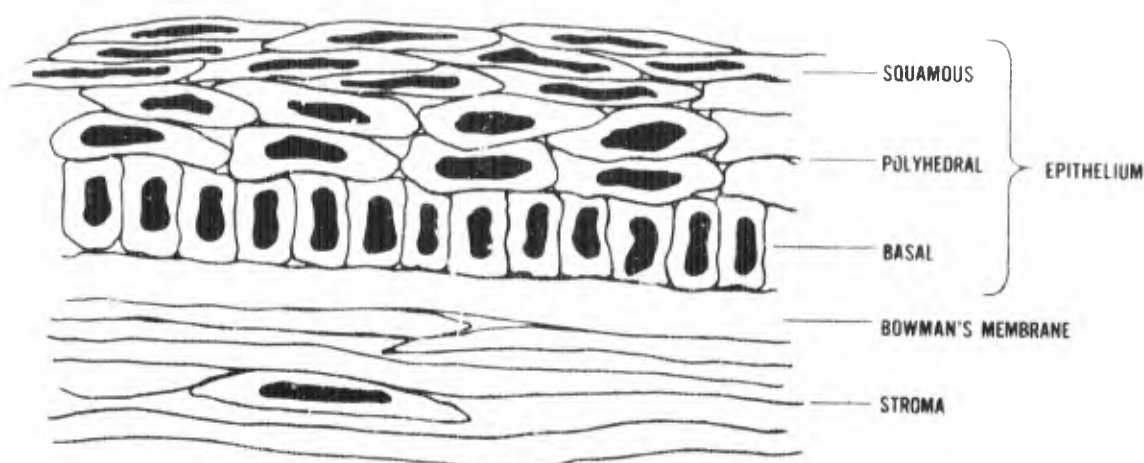


Figure 8. Transverse section of corneal epithelium.

three layers of squamous cells, more elongated than the polyhedral cells, also run parallel to the corneal surface.

Basal cell mitosis generates the other epithelial cells. After being formed the cells are gradually pushed upward to the corneal surface, changing in shape and orientation during this process. Upon reaching the surface the cell dies (in a day or so) and decomposes, the debris being sloughed off into the tear layer. The average cell life is approximately 6 days.

Although the cells change their positions and shapes during the 6-day lifetime, the molecular composition remains basically unchanged. It may be anticipated, therefore, that the basal, polyhedral, and squamous cells will all show the same sensitivity to UV radiation.

The corneal epithelium exhibits very great recuperative powers. Even if the entire epithelium is stripped off, a complete new layer of basal cells may be regenerated within 24 hours, by multiplication of the peripheral conjunctival cells. In several weeks this single layer develops into a complete epithelium.

Although no repair mechanism, per se, has been identified in the epithelium, the normal cell-replacement rate must be taken into account when considering repeated UV exposures over a period of time. Since the average 6-day cell life involves traversing five or six layers, the cell spends roughly 1 day in each layer. Thus, threshold radiation damage restricted to the outermost layer of cells would be obscured within 1 day by the normal cell-replacement progression. Damage penetrating the 6 epithelial layers could appear "repaired" in approximately

6 days by the same process. If, in addition, there is a repair mechanism operative within individual cells, the observed repair rate may be more rapid than the replacement rate. Any cellular repair mechanism identified in damaged epithelial tissue would provide invaluable information regarding the nature of the molecular lesions which lead to observed macroscopic damage.

The stroma accounts for 90% of the cornea's thickness. A cross-sectional view (Fig. 8) shows the stroma made up of lamellae, or flat sheets, 1.5μ - 2.5μ thick and running parallel to the corneal surface. The lamellae are composed of collagen fibres which run parallel to each other within any given sheet. Adjacent layers have their fibres oriented in perpendicular directions. The human cornea contains over 200 such overlapping lamellae.

An occasional cell is found lying within the lamellae. These cells are usually flattened, with enlarged nuclei, and have "branches" connecting to neighboring cells. The stroma, however, is basically a structural medium, and observable radiation damage appears to involve disruption of the collagen fibres rather than the occasional cell. Destroyed collagen fibres can be replaced in the stroma, but since this does not necessarily occur with the proper orientation, permanent opacity or scarring results.

Bowman's and Descemet's membranes are extensions of the stroma and also composed mainly of collagen fibres; the chief difference between the three layers lies in the ordering of the fibres within each layer. The endothelium is a single layer of cells with molecular composition similar to the epithelium of the cornea and, hence, fairly well shielded from the most damaging forms of radiation.

For considering UV-radiation damage, we may think of the cornea as composed of two layers: the epithelium, or cellular layer, and the stroma (including Bowman's and Descemet's membranes), or structural layer. Epithelial damage is apparently completely reversible, while stromal damage results in permanent scarring. The action spectrum of Figure 4 shows the wavelength dependence for epithelial damage. Little is known about the wavelength dependence or stromal damage or for that matter about the threshold for stromal damage at any wavelength.

MOLECULAR COMPOSITION OF THE CORNEA

The basal, polyhedral, and squamous cells of the epithelium have a common parenthood and, hence, a common molecular composition. Water makes up 80% of the epithelium. The dry material composition is (7):

75%	protein
11%	lipid (fat)
5%	glycogen (carbohydrate)
3%	nucleic acid
1%	various salts

The stroma, also 75%-80% water, has a dry material composition of (12):

90%	protein
4%	polysaccharide (carbohydrate)
1%	lipid (fat)
1%	various salts

Of the stromal protein, some 70% is the collagen making up the array of fibres. The stroma has only a trace of nucleic acid (<0.1%), localized in the few cells interspersed within the collagen lamellae.

In view of the function of the cornea, it is not surprising that it contains no pigments which absorb visible light. UV absorption by the cornea is due to certain constituents of the proteins and nucleic acids. Since nucleic acid is negligible in the stroma, absorption in that layer is due solely to protein. In the epithelium, the nucleic acid absorption is comparable to protein absorption over much of the UV range (despite the 25:1 ratio of protein to nucleic acid).

To more fully characterize the interaction of UV radiation with the cornea, a brief review is presented of the molecular composition and absorption properties of proteins and nucleic acids. For further information the reader is referred to several standard texts (3, 8, 13, 16).

A protein is a linear polymer of amino acids. The repeat sequence is illustrated in Figure 9. Some 20 amino acids are commonly found in proteins, differing only in the nature of the side chain R (Fig. 9). Of the 20, three amino acids are aromatic in nature and account for the UV absorption of proteins. The structures of these three chromophores are shown in Figure 10. Several other amino acids begin to absorb in the vicinity of 200 nm. In the vacuum UV all amino acids and the peptide bonds linking them together absorb quite strongly.

The absorption spectra of the aromatic amino acids are shown in Figure 11. The absorption spectrum of serum albumin (Fig. 12) is representative of almost all naturally occurring proteins. From the spectra of the aromatic amino acids a protein absorption curve can be constructed. The major features of the protein spectra (the maxima near 275 nm and 225 nm

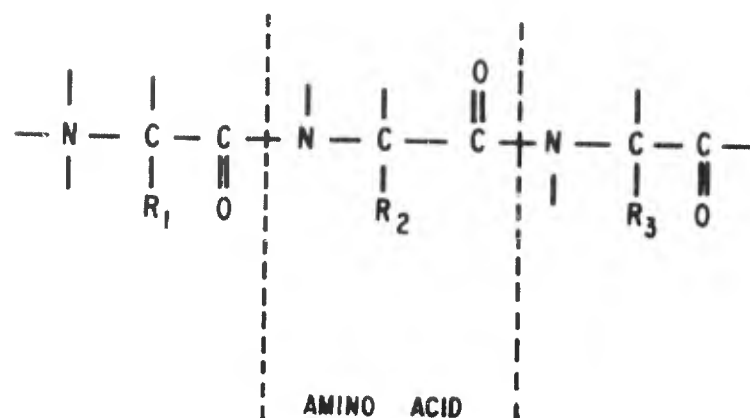


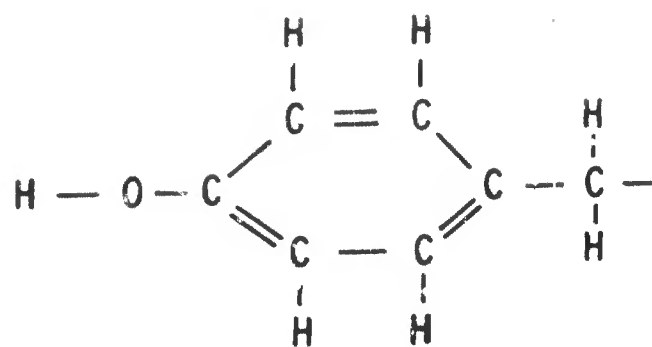
Figure 9. Molecular structure of protein.

and the minimum near 250 nm) vary slightly from protein to protein depending on the relative abundance of the aromatic amino acids in each case.

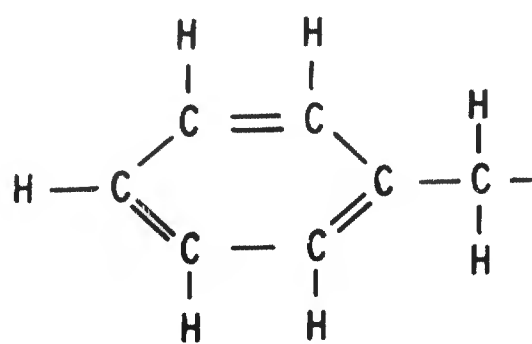
A nucleic acid chain is a linear polymer of monomer units called nucleotides. As shown in Figure 13, a nucleotide consists of a sugar, a phosphate group, and a base which is either a purine or pyrimidine derivative (Fig. 14). The sugar and phosphate are transparent above 200 nm, and only the base accounts for the DNA absorption spectrum shown in Figure 12. Several kinds of nucleic acids are found in the cell, but all have similar bases with similar absorption spectra. Therefore, the DNA curve of Figure 12 represents the absorption of all cellular nucleic acids.

The UV-absorbing species in the cornea have been identified as the aromatic amino acids of proteins and the bases of nucleic acids. To show that these components satisfactorily explain the observed absorption spectra for the epithelium and the entire cornea, theoretical absorption curves can be constructed. (See Appendix A.) The calculated and observed absorption spectra for the corneal epithelium are compared in Figure 15. A close fit is obtained over the entire far UV. The fact that the observed and predicted curves are not quite parallel and cross at 290 nm is probably due to choosing a particular protein containing a slightly different ratio of aromatic amino acids than the average composition for the cell.

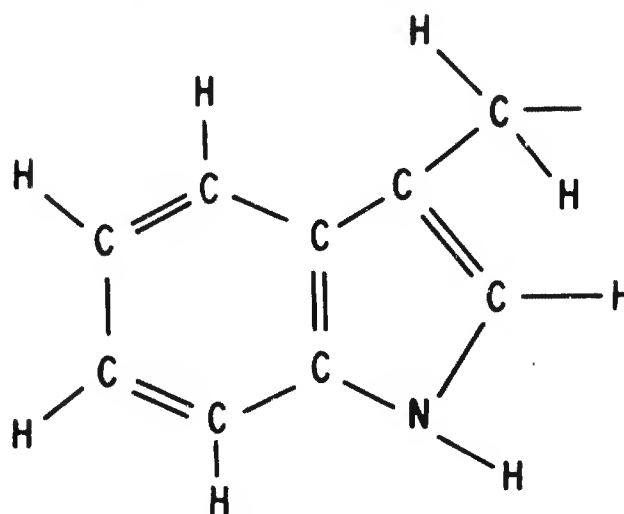
The absorption spectrum for the entire cornea (Fig. 2) is reproduced by merely considering the absorption of a 500 μ thick protein solution of the proper concentration ($\approx 20\%$).



TYROSINE



PHENYLALANINE



TRYPTOPHAN

Figure 10. Aromatic amino acids.

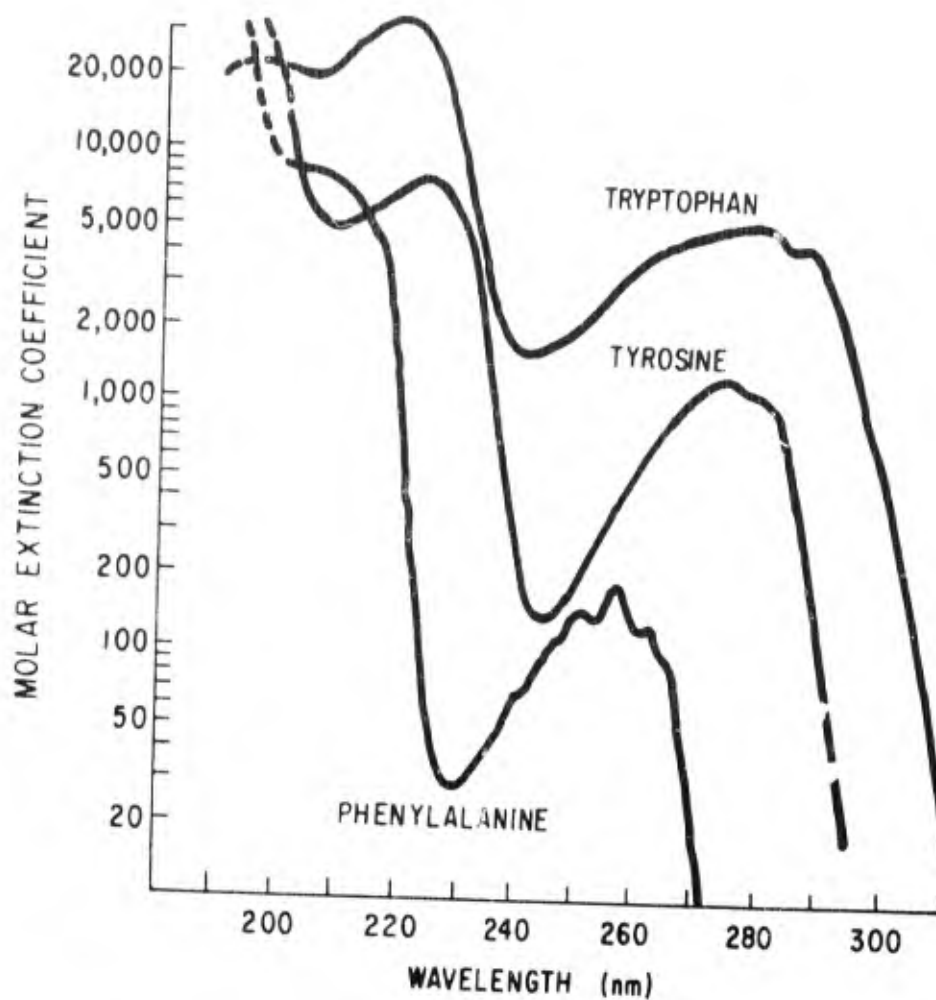


Figure 11. Absorption spectra of the aromatic amino acids.

This shows a steep rise in absorption beginning at about 320 nm and reaching 100% near 280 nm.

The origin of the residual absorption of the cornea above 320 nm is not clear. The extinction coefficients of proteins and nucleic acids are very low above 320 nm and have not been measured accurately. In the cornea there are undoubtedly trace amounts of many other molecules which may absorb in the 320- to 400-nm range. Because of the weak absorption, relatively high levels of incident radiation are required to cause observable damage in this wavelength range. Whether the dominant mechanism for damage is photochemical in nature or not is open to speculation.

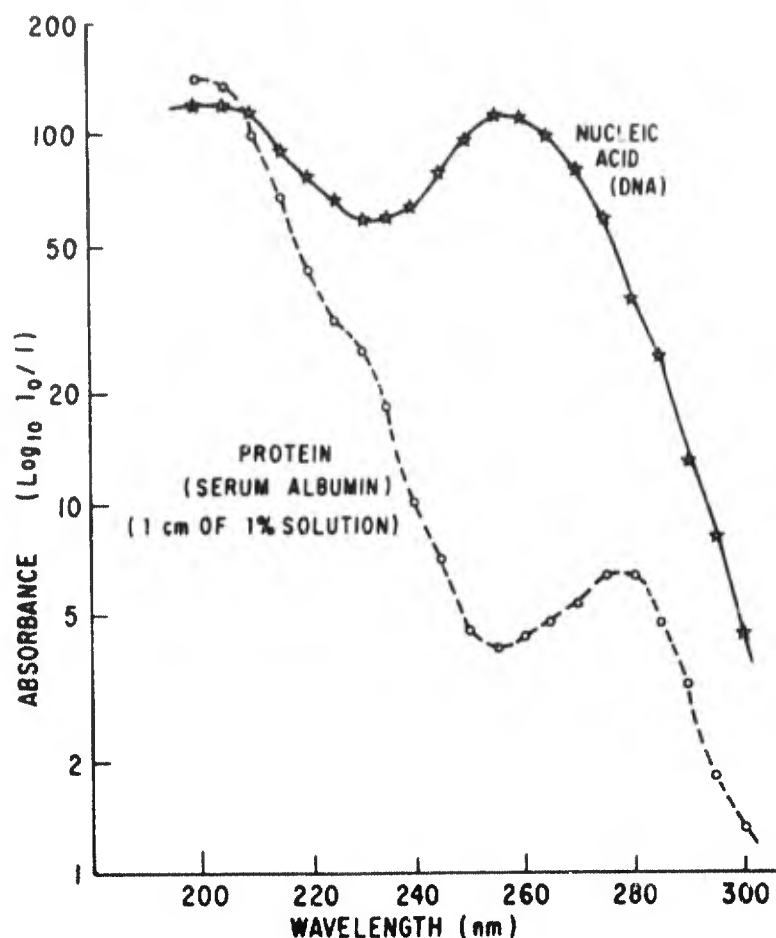


Figure 12. Absorption spectra of biological macromolecules.

Since the absorption coefficients of proteins and nucleic acids vary considerably with wavelength in the far UV, the fraction of absorbed energy actually deposited at protein or nucleic acid sites also strongly depends on wavelength. However, the relative absorptions of each species at any wavelength are readily calculated as detailed in Appendix A. Reciprocals of these absorptions, which for lack of a better term will be called relative transmissions, are plotted in Figure 16. The reciprocals are chosen so that the curves can be compared to the action spectrum for photokeratitis, also shown in Figure 16. While proteins continue to absorb more incident energy as the wavelength is lowered below 260 nm, the nucleic acid sites begin to absorb less (despite their higher extinction coefficients at shorter wavelengths) because of the greater shielding effects of the proteins. Interestingly, the action spectrum for photokeratitis (except for the anomalous

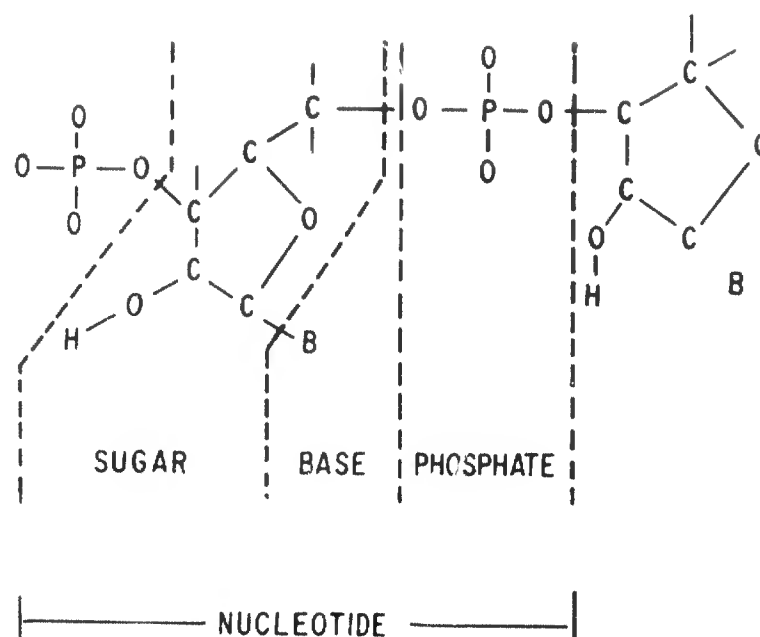


Figure 13. Molecular structure of nucleic acid.

peak at 250 nm) roughly parallels the nucleic acid relative-transmission curve. This, taken together with many in vitro and in vivo studies of photochemical damage to biological systems (11, 15), indirectly supports identifying nucleic acids (in particular, the DNA of the chromosomes) as the primary sites for photochemical damage leading to cell death.

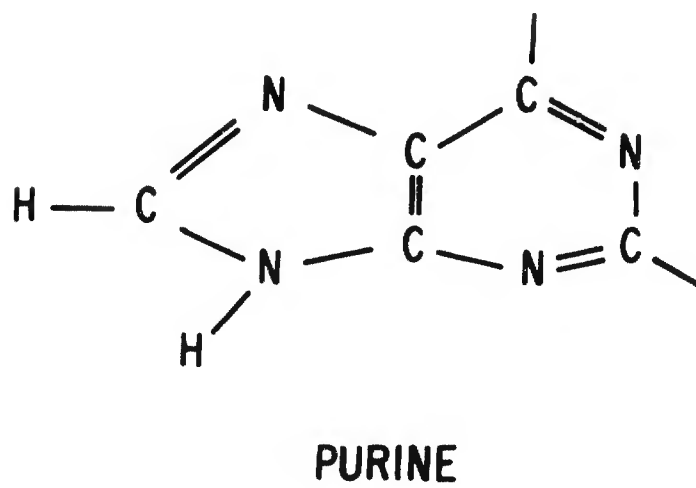
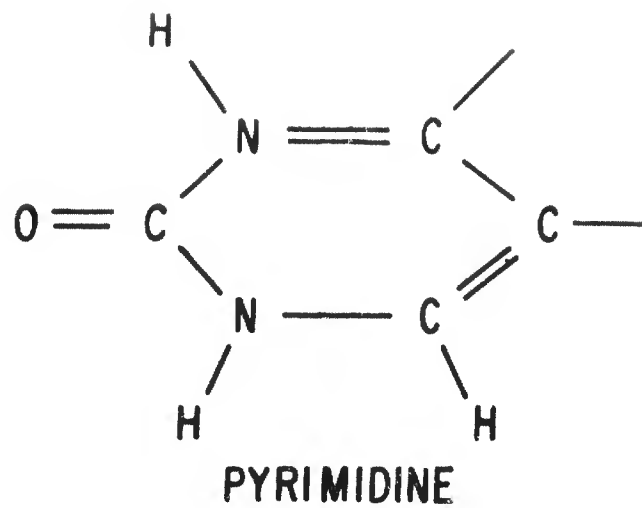


Figure 14. Nucleic acid bases.

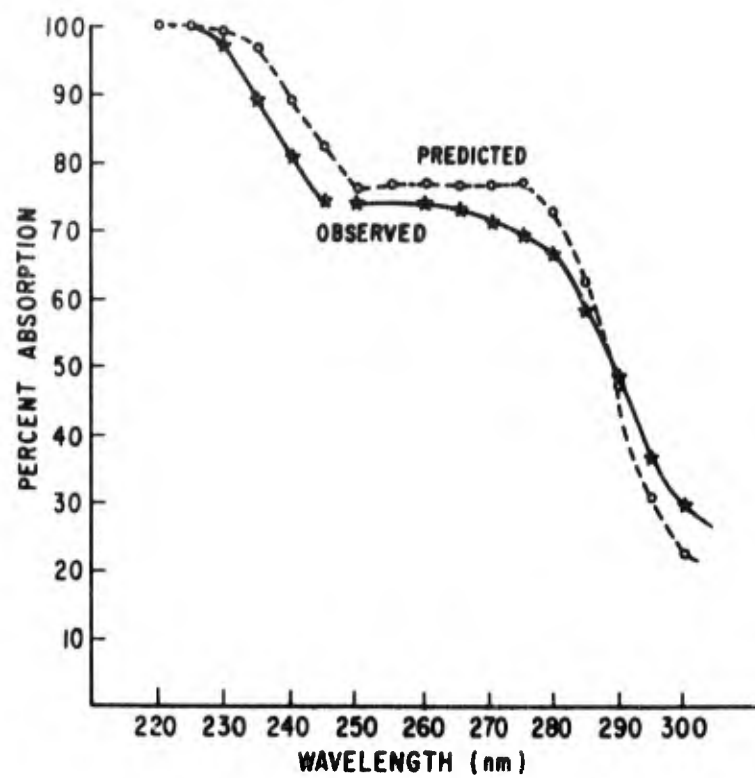


Figure 15. Absorption spectrum of corneal epithelium (rabbit).

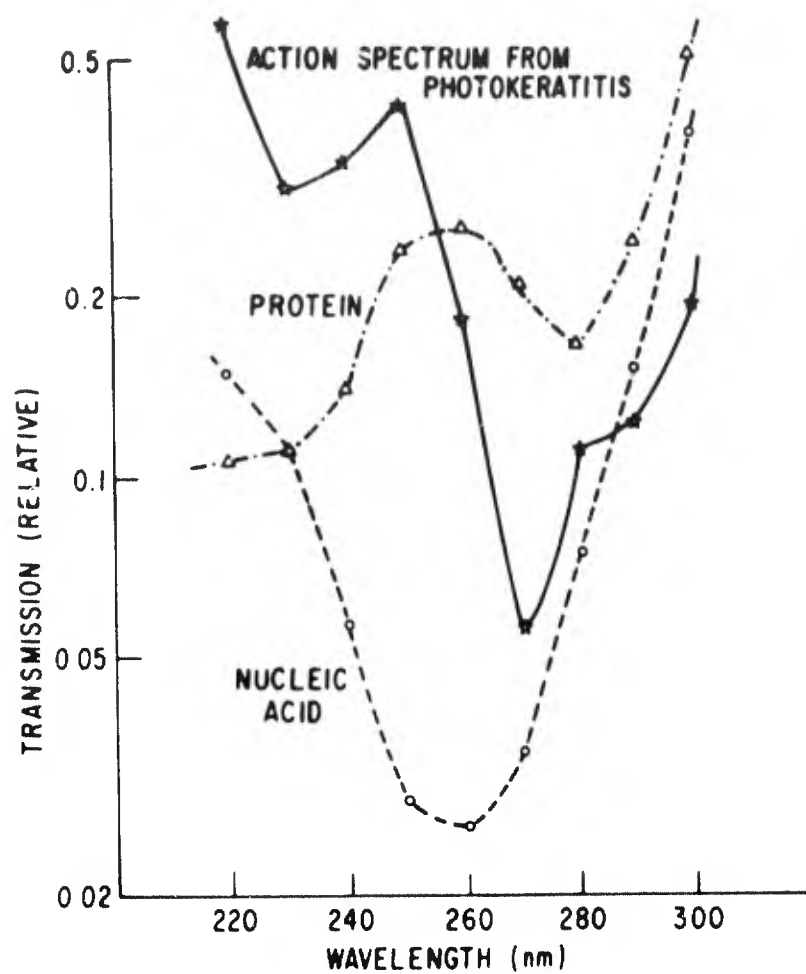


Figure 16. Relative transmissions of proteins and nucleic acids of the corneal epithelium.

REFERENCES

1. Bachem, A. Ophthalmic ultraviolet action spectra. *Am J Ophthal* 41:969 (1956).
2. Boettner, E. A. Spectral transmission of the eye. Final Report, Contract AF41(609)-2966, Project No. 6301, University of Michigan, Ann Arbor, Mich. (July 1967).
3. Chargaff, E., and J. Davidson. The nucleic acids. New York: Academic Press, 1955.
4. Cooper, G. F., and J. G. Robson. The yellow colour of the lens of man and other primates. *J Physiol* 203:411 (1969).
5. Davson, H. The physiology of the eye, 3d ed. New York: Academic Press, 1972.
6. Ebberts, R. W. Laser Effects Branch, USAFSAM, Brooks AFB, Tex. Personal communication, 1973.
7. French, R. C., and Z. Duma. Studies on protein metabolism of the cornea. *Can J Biochem Physiol* 41:1005 (1963).
8. Haynes, R. H., and P. C. Hanawalt (eds.). The molecular basis of life: Readings from Scientific American. San Francisco: Freeman, 1968.
9. Kinsey, V. Spectral transmission of the eye to ultraviolet. *Arch Ophthal* 39:508 (1948).
10. Last, R. J. Wolff's anatomy of the eye and orbit, 6th ed. Philadelphia: W. B. Saunders, 1968.
11. McLaren, A., and D. Shugar. Photochemistry of proteins and nucleic acids. New York: Pergamon Press, 1964.
12. Maurice, D. M., and M. V. Riley. The cornea. In C. Graymore (ed.). Biochemistry of the eye. New York: Academic Press, 1970.
13. Neurath, H., and K. Bailey (eds.). The proteins. New York: Academic Press, 1955.
14. Pitts, D. G., et al. The effects of ultraviolet radiation on the eye. SAM-TR-69-10, Feb. 1969.
15. Smith, K., and P. Hanawalt. Molecular photobiology. New York: Academic Press, 1969.
16. Steiner, R. F. The chemical foundations of molecular biology. Princeton: D. van Nostrand, 1965.

APPENDIX A

MOLECULAR ABSORPTION IN THE CORNEAL EPITHELIUM

The absorbance (A) of a solution of concentration c and optical path b is defined as follows:

$$A = \epsilon bc = \log_{10}(I_0/I)$$

where I_0 is the intensity of the incident radiation and I is the intensity of the transmitted radiation. ϵ is the molar extinction coefficient provided that c is in units of moles per liter and b is in units of centimeters. The quantity A is also referred to as "optical density," "extinction," and "absorbancy."

If the molecular weight of the absorbing species is unknown, it is standard procedure to report to absorbance of a 1% (by weight) solution with a 1-cm optical path. This absorbance is symbolized by $A_{1\%}^{1\text{cm}}$.

For a solution with more than one absorbing species, the absorbances are additive.

The absorbing species of the corneal epithelium have been identified as the aromatic amino acids of proteins and the bases of nucleic acids. The absorption spectra shown in Figure 12 represent the absorption spectra for all proteins and nucleic acids in the epithelium. The values of $A_{1\%}^{1\text{cm}}$ for these species are presented in Table A-1.

The proteins and nucleic acids are localized in particular regions of the epithelial cells. However, for purposes of calculating the absorbance of this layer on a macroscopic scale, the epithelium is assumed to be a homogeneous mixture of protein and nucleic acid. The absorbance of the layer is thus:

$$A = A_p + A_n = \epsilon_p bc_p + \epsilon_n bc_n$$

where the subscripts p and n refer to protein and nucleic acid, respectively, and b is the thickness of the epithelium. The quantities reported in the second and third columns of Table A-1 are A_p and A_n for 1% solutions, 1 cm thick. The thickness of the epithelium is taken as 50 μ . The composition of the epithelium is 80% (by weight) water; of the dry material, 75% is protein and 3% nucleic acid. The epithelium, therefore, is

taken to be a solution with 15% protein and 0.6% nucleic acid. The absorbance of this layer is thus:

$$\begin{aligned} A &= A_p + A_n = (A_p)_{1\text{cm}}^{1\%} \times 15 \times 5 \cdot 10^{-3} + (A_n)_{1\text{cm}}^{1\%} \times 0.6 \times 5 \cdot 10^{-3} \\ &= 0.075 (A_p)_{1\text{cm}}^{1\%} + 0.003 (A_n)_{1\text{cm}}^{1\%} \end{aligned}$$

The calculated absorbance is shown in the fourth column of Table A-1. The percent absorption (%Abs), which is equal to $100 (I_0 - I)/I_0$, is shown in the last column and plotted along with the experimental absorption spectrum in Figure 15.

It is interesting to calculate the fraction of absorbed energy deposited with each absorbing species at any given wavelength. The fraction f_i absorbed by the i^{th} species is, in general:

$$f_i = \frac{A_i}{\sum_j A_j}$$

where the summation is over all absorbing species in the solution. The fractions f_p and f_n for the protein and nucleic acid components of the epithelium are reported in Table A-2. The relative absorption of the i^{th} component will be the product of the percent absorption of the epithelium at any wavelength and the corresponding fraction f_i at the wavelength. These products are listed along with their reciprocals in Table A-2. The reciprocals, or relative transmissions, are plotted in Figure 16, where they are compared with the action spectrum for photokeratitis.

TABLE A-1. ABSORPTION OF THE CORNEAL EPITHELIUM

Wavelength	Solution absorbances		Epithelial absorption	
(nm)	$(A_p) \frac{1\%}{1\text{cm}}$	$(A_n) \frac{1\%}{1\text{cm}}$	$A=A_p+A_n=\log(I_0/I)$	%Abs
220	42	76	3.38	99.96
225	31	66	2.52	99.7
230	26	58	2.12	99.2
235	18	59	1.53	97.1
240	10	63	.939	88.5
245	7.0	77	.756	82.5
250	4.5	94	.620	76.0
255	4.0	111	.636	76.9
260	4.3	108	.647	77.5
265	4.7	97	.644	77.3
270	5.3	79	.635	76.8
275	6.3	58	.647	77.5
280	6.3	35	.578	73.6
285	4.7	25	.428	62.8
290	3.2	13	.279	47.4
295	1.8	8.0	.159	30.7
300	1.3	4.4	.113	22.9

TABLE A-2. RELATIVE ABSORPTIONS OF PROTEIN AND NUCLEIC ACID COMPONENTS OF EPITHELIUM

Wave-length	Fractional absorbances		Relative absorptions		Relative transmissions	
(nm)	f_p	f_n	$f_p \times \% \text{Abs}$	$f_n \times \% \text{Abs}$	$1/(f_p \times \% \text{Abs})$	$1/(f_n \times \% \text{Abs})$
220	.933	.067	93.3	6.70	.011	.149
225	.922	.078	91.9	7.78	.011	.129
230	.918	.082	91.1	8.13	.011	.123
235	.884	.116	85.8	11.3	.012	.089
240	.799	.201	70.7	17.8	.014	.056
245	.694	.306	57.3	25.2	.018	.040
250	.545	.455	41.4	34.6	.024	.029
255	.474	.526	36.5	40.4	.027	.025
260	.499	.501	38.7	38.8	.026	.026
265	.548	.452	42.4	34.9	.024	.029
270	.626	.374	48.1	28.7	.021	.035
275	.731	.269	56.7	20.8	.018	.048
280	.818	.182	60.2	13.4	.017	.075
285	.825	.175	51.8	11.0	.019	.091
290	.860	.140	40.8	6.64	.025	.151
295	.849	.151	26.1	4.64	.038	.216
300	.881	.119	20.2	2.73	.050	.367